Phononic Crystal Waveguides for Structural Health Monitoring Applications

FRANCESCO CIAMPA

ABSTRACT

This paper reported applications of 3D printed acrylic phononic crystal (PC) waveguide transducers for application within NEWS methods. Experimental evidence has shown to support the mathematical formulation of the imaginary component of the complex wavenumber shift used in the design of circular PCs with sinusoidally corrugated profiles. Experimental evidence has also supported the existence of band gaps resultant from the destructive interference of both incident and reflected fundamental Lamb waves at specific frequency band gaps. These stop bands allow PC transducers to possess their unique feature of natural filters undesired frequencies, for example those originated from the ultrasonic equipment. NEWS tests have finally shown that second harmonic waves generated from the contact surfaces of micro-cracks could be accurately detected with PC waveguide transducers used during ultrasonic transmission. This technology can be applied, in future, for more accurate, automatable, and simpler microcrack detection.

INTRODUCTION

Nonlinear ultrasonic GW methods – also known as nonlinear elastic wave spectroscopy (NEWS) techniques - measure nonlinear wave effects including harmonics (multiples), sub-harmonics (sub-multiples) and sidebands (modulation) of one or more excitation frequencies [1], [2], which are caused by the vibration-induced nonlinear contact (e.g., rubbing" and "clapping") at crack interfaces, with typical driving frequencies ranging between 100 kHz and 500 kHz. However, NEWS testing is generally affected by "undesired" harmonics caused by the ultrasonic equipment, which are comparable in magnitude with those generated by the crack. This poses a major challenge for the full-scale use of NEWS methods: *the need to develop "electronic-free" signal filters to enhance the detection of nonlinear wave effects generated by the damage*.

Phononic crystals (PC) are periodic arrangements of elementary cells, whose structure - often containing inclusions or cavities - induces non-conventional dispersion properties [3]. A unique peculiarity of PCs is that through the Bragg-scattering or the local resonance effects they can be designed to suppress the propagation of ultrasonic

Francesco Ciampa, Dep. of Mechanical Engineering Sciences, University of Surrey, Guildford, GU27XH, UK.

waves in tailored frequency ranges known as band gaps (BGs) or stop bands [4]. Conversely, wave propagation is supported outside these BG frequencies. Research studies have been focused on enhancing the spatial and dynamic properties of PCs by designing BGs for noise absorption, acoustic lenses, and acoustic diodes [5]. However, PCs typically require substantial modification (e.g., holes and inclusions) of the test component to create frequency band gaps, thus affecting the structural integrity. Ciampa et al. [6] and Sherwood et al. [7] proposed the first prototype of phononic crystal waveguide transducer, which consisted of a traditional piezoelectric sensor bonded onto a 3D-printed circular structure made of Acrylonitrile Butadiene Styrene (ABS) with sinusoidal boundary profiles. Authors also created the analytical model predicting band gaps in PC waveguides, which relies on a perturbative couple-mode theory of guided Lamb wave propagation in isotropic PCs with periodic gratings. It was shown that stop bands in PC waveguides can be tuned by varying material and geometrical design parameters of PCs such as the wavelength, corrugation depth, thickness and diameter. Recently, Li et al. [8] developed PCs for non-destructive testing applications.

The main contribution of this paper is to further enhance the stop band features of PC waveguide transducers by implementing novel and more accurate 3D-printing fabrication methods of PCs and provide the first experimental evidence of second harmonic detection in damaged materials.

FABRICATION OF PC WAVEGUIDE TRANSDUCERS

Thermoplastic polymers were chosen as the manufacturing material of PC transducers as they (i) can be rapidly fabricated with cost-effective additive manufacturing (3D-printing) processes, (ii) are characterised by lightweight and high mechanical strength and (iii) induce low phase velocities of Lamb waves at the interface between the PC waveguide and the host sample, in accordance with the Snell's Law [9]. Polyjet technology was employed to fabricate PCs. This 3D printing method relies on material photopolymerisation with UV light and provides high vertical accuracy up to ~0.01 mm [10]. Such high vertical resolution enables dramatic precision in the fabrication of sinusoidal grooves. Acrylic (VeroClear) type filaments were used as the thermoplastic material in the Polyjet technology. PCs were printed using the Stratasys Objet260 3D-printer. Sinusoidal profiles in each PC were printed to 16 μm layer resolution and, after printing, parts were soaked in an alkali bath to remove the SUP705 soluble support material that was used during the manufacture. The imaginary corrugation induced wavenumber shift, $\beta''(f)$, was calculated for the design parameters reported in Table 1 and Figure 1 according to the following formula,

$$\beta(f) = \frac{1}{2}\left[\frac{2\pi}{\Lambda(2f_0)} - (k_A + k_S)\right] + \frac{1}{2}\sqrt{\left[\frac{2\pi}{\Lambda(2f_0)} - (k_A + k_S)\right]^2 - 4C_A C_S\left(\frac{\pi\epsilon}{\Lambda(2f_0)}\right)^2} = \beta'(f) + i\beta''(f) \quad (1)$$

where $k_S(f)$ and $k_A(f)$ are the symmetric and antisymmetric wavenumbers, 2ϵ is the corrugation dept, coefficients $C_{S,A}$ are functions of the material and geometrical features of the PC such as the diameter D and average thickness $2h$ (see ref. [6]), and the corrugation period is obtained from $\Lambda(2f_0) = \frac{2\pi}{[k_S(2f_0)+k_A(2f_0)]}$.

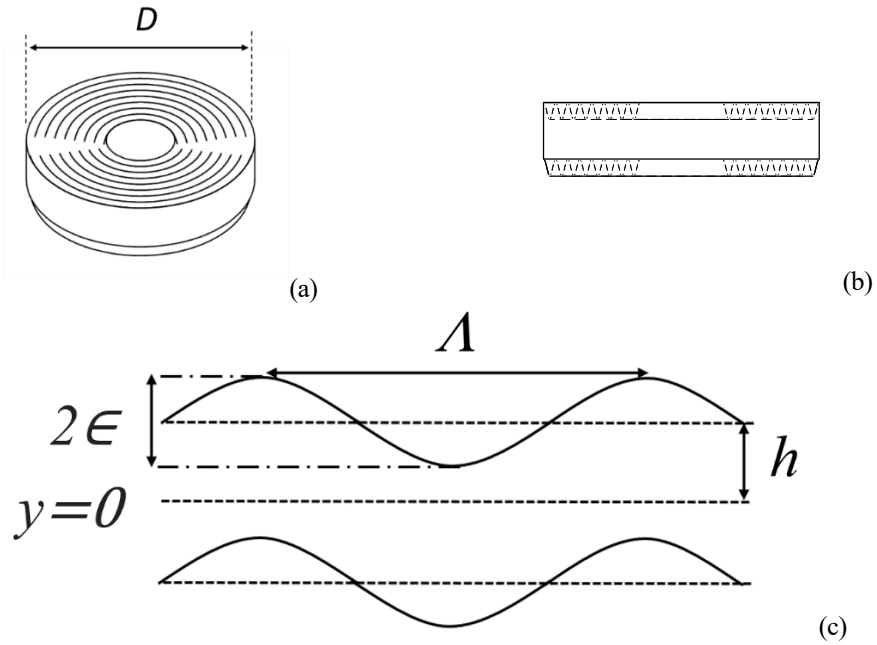

Figure 1. Schematic representation of the PC waveguide structure (a) and its side view (b). Design parameters of the corrugated PC waveguide (c).

Two fundamental frequencies were selected for the design of PC structures, i.e., f_0 = 100 kHz and 150 kHz. Therefore, PC waveguide transducers associated with these two input frequencies were named as PC100 and PC150, respectively.

TABLE I. DESIGN PARAMETERS OF PC TRANSDUCERS

PC Structure	f_0 **(kHz)**	$2h$ **(mm)**	Λ **(mm)**	2ϵ **(mm)**	N	D **(mm)**
PC100	100	10	2.10	2	8	48.0
PC150	150	10	1.38	2	8	33.6

Spectral ranges with $\beta''(f) = 0$ are the passband frequencies in which GWs are not filtered out and are free to propagate. In the phononic band region, instead, $\beta''(f) \neq 0$ and the ultrasonic wave propagation is inhibited. As show in the dispersion curves of Figure 2, the passband region for the acrylic PC100 ranged from 20 kHz to 150 kHz and from 60 kHz to 180 kHz for PC150. Therefore, second harmonic waves propagating at 200 kHz and 300 kHz for PC100 and PC150, respectively, resulted in the stop band region of each PC waveguide and their propagation was suppressed.

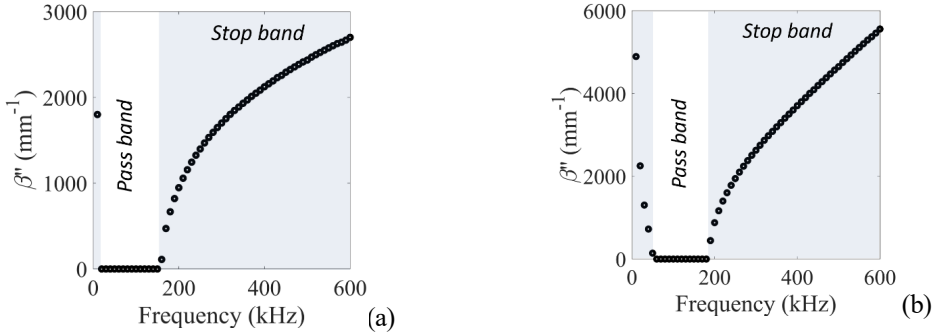

Figure 2. Dispersion curves of PCs with f_0 = 100 kHz - PC100 (a), and f_0 =150 kHz - PC150 (b).

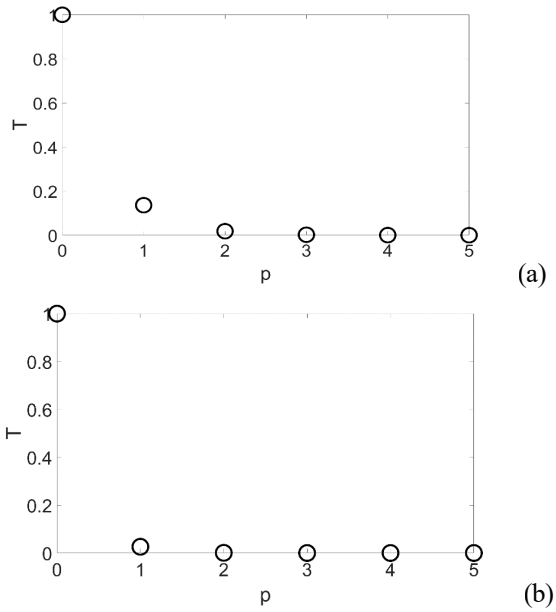

Figure 3. Transmission curves of PC100 (a) and PC150 (b).

The number of sine wave shaped corrugations, N, upon which the stop band region becomes effective (see Table 1) was calculated through the transmission coefficient T [6], [7], which provides the distance required for the ultrasonic wave intensity to be attenuated. As shown in Figure 3, an ideal value of $p = 2$ periods is sufficient for both PC100 and PC150 to reduce nearly 100% of the elastic energy at the stop band. Therefore, a safety margin of four was used for the design of PCs and $N = 8$ grooves were used in each PC structure.

RESULTS AND DISCUSSIONS

A 3 mm thick 1050A aluminium plate was used as the test piece to which PC100 and PC150 waveguide transducers were bonded at distance of 100 mm from their geometric centre. PZT sensors with a diameter of 6.5 mm and thickness of 0.3 mm were attached centrally on the top surface of each PC waveguide structure using an epoxy resin. Two further PZT sensors, namely PZT1 and PZT2, were glued directly on the aluminium specimen for NEWS comparison tests far away 40 mm from PCs. These transducers could be used as both transmitters and receivers [see Figure (4)].

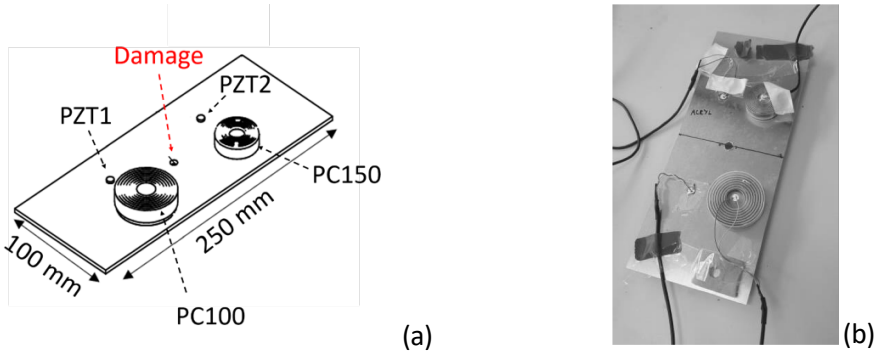

Figure 4. Schematic of transducers' configuration (a) and photograph of the experimental set up (b).

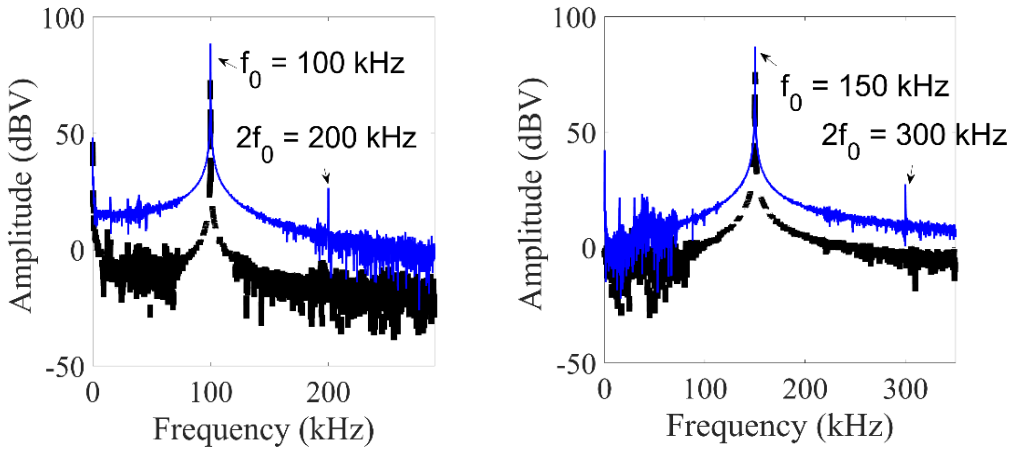

Figure 5. Frequency spectra using PC100 (a) and PC150 (b) waveguide transducers.

For the ultrasonic signal transmission in all NEWS tests, 15 cycles long sine wave bursts $s(t) = M_0\, H(t) \sin(2\pi f_0 t)$ enclosed in a Hanning window $H(t)$, with M_0 being the input amplitude, were transmitted by both PZT and PC waveguide transducers. Signal received by PZTs were sampled at 2 MHz with an acquisition window of 5 ms. In order to experimentally analyse the second harmonic filtering capabilities of the proposed acrylic PC waveguide transducers, periodic burst signals at the driving frequencies f_0 = 100 kHz and 150 kHz were emitted by PC100 and PC150, respectively, with an input voltage M_0 = 75 V. Whilst the ultrasonic signal emitted by PC100 was recorded by PZT 2, the waveform emitted by PC150 was measured by PZT1. For comparison purposes, the same input signals were transmitted and received between the two PZT sensors bonded directly onto the aluminium plate. Time histories were averaged 20 times for each input frequency to improve the signal-to-noise ratio of measured waveforms. Figure 5 shows the spectral responses with (black dashed line) and without (blue continuous line) the use of PC waveguide transducers.

In order to evaluate the pass band effect of acrylic PC waveguide transducers, input frequencies, f_0, whose second harmonic wave, $2f_0$, lie within the pass band region were investigated. These frequencies are characterised by the condition $\beta''(f_0) = 0$ and $\beta''(2f_0) = 0$ as for Eq. (1) and the dispersion curves of Figure 2. The aluminium sample was still at its undamaged state, so that the second harmonic wave was only caused by the ultrasonic equipment. Driving frequencies f_0 = 60 kHz and 80 kHz were selected and transmitted through PC100 and PC150 waveguide transducers, respectively, which both lie within the pass band spectrum along with their associated second harmonic frequencies $2f_0$ = 120 kHz and 160 kHz [Figures 2(a-b)]. As before, the receiver transducers PZT2 and PZT1 were used to acquire the material ultrasonic response. It can be seen from Figure 6(a) that the second harmonic amplitude of 3.26 dBV was measured at 120 kHz with PC100, thus supporting the band gap hypothesis that f_0 and $2f_0$ were allowed to pass without being filtered out as they lay within the pass band. The same occurred for PC150 where a second harmonic of 3.12 dBV was detected at 160 kHz [Figure 6(d)].

Figure 7 illustrates the recorded peak amplitudes of second harmonic frequencies, $2f0$, using PC100 (dashed line) and PC150 (continuous line) as emitter transducers. The second harmonic response in the undamaged aluminium sample is in agreement with

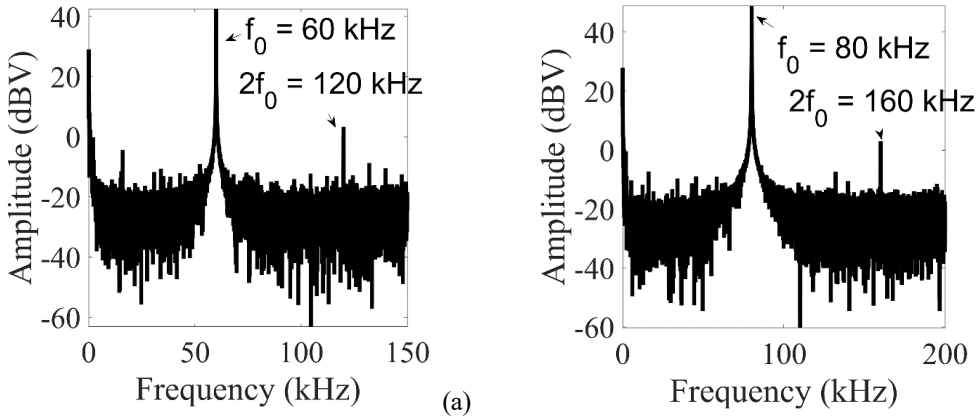

Figure 6. Frequency spectra obtained by transmitting a burst signal at f_0 = 60 kHz with PC100 (a) and f_0 = 80 kHz with PC150 (b).

the stop-band results of Figure 2 for both PC structures, thus further validating the analytical predictions [Eq. (1)]. This third set of NEWS tests involved the creation of few mm cracks into the aluminium test sample that triggered second harmonic waves caused by the interaction of GLWs with the material damage. A 7 mm hole was firstly drilled in the centre of the aluminium sample, equidistant from each PC waveguide transducer. Then, two 3 mm notches were sawn into either side of the hole and small cracks were initiated at the ends of notches by hammering a razor blade into the aluminium to form cracks 1 mm long (Figure 8).

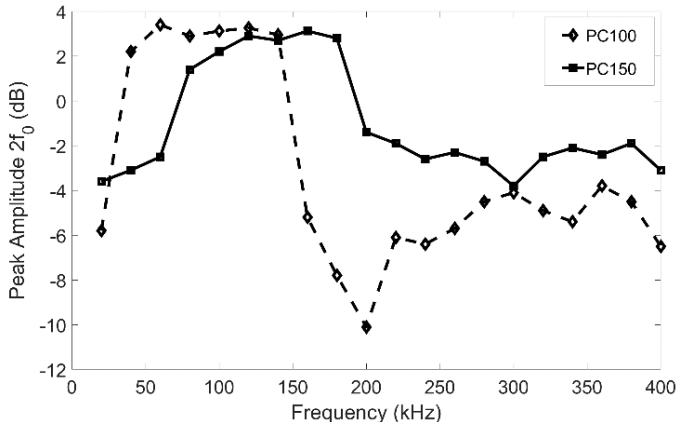

Figure 7. Peak amplitudes the second harmonic frequency using acrylic PC100 (dashed line) and PC150 (continuous line) as transmitter transducers. The input amplitude was 75 V.

Figure 8. Photograph of the 1 mm long crack created on the aluminium sample.

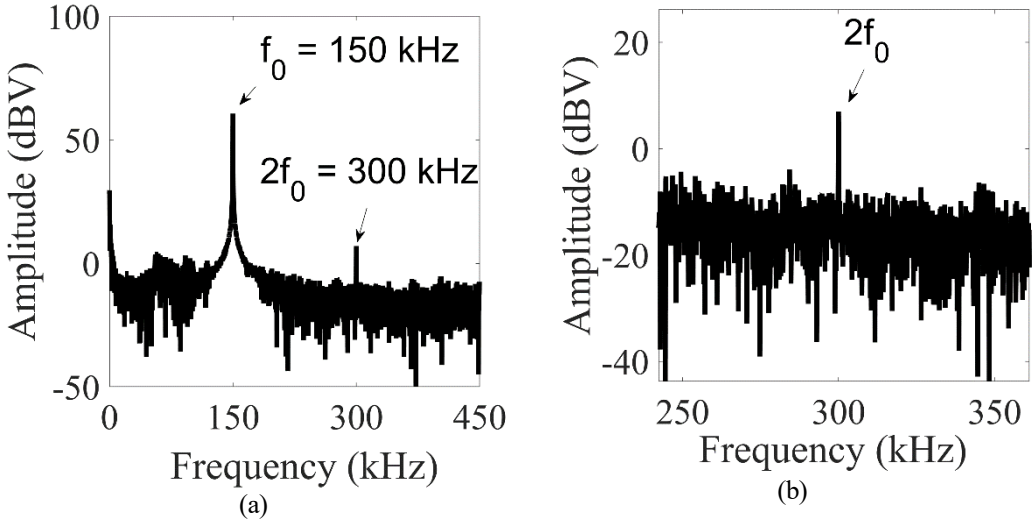

Figure 9. Experimental material response measured by the PZT1 receiver sensor using a burst input signal emitted by PC150 in the damaged plate (a) and enhanced view of the second harmonic frequencies $2f_0$ = 300 kHz (b).

The PC150 waveguide transducer with f_0 = 150 kHz was used in NEWS tests and the nonlinear material response was measured using the PZT1 receiver sensor. As in previous experiments, the input amplitude was set equal to 75 V. Figure 9 shows the frequency spectrum measured by PZT1 in which a second harmonic frequency at $2f_0$ = 300 kHz is clearly visible with an amplitude of 6.8 dBV.

CONCLUSIONS

Second harmonic filtering experiments with the undamaged aluminium plate showed that PC150 successfully suppressed the second harmonic frequency caused by the ultrasonic equipment. NEWS tests on the damaged aluminium sample further confirmed the effectiveness of 3D-printed PC waveguide transducers in suppressing nonlinearities caused by the ultrasonic instrumentation and enhancing the detection of second harmonic nonlinear effects.

REFERENCES

1. Van Den Abeele, K.E., et al. NDT & E International, 34(4), 239-248, 2001.
2. Antonaci, P., et al. Cement and Concrete Research, 51, 96-103, 2013.

3. Liang, B., et al. Nature materials, 9(12), p.989, 2010.
4. Maldovan, M. Nature, 503(7475), p.209, 2013.
5. Klein, L., Joseph, Y. and Kröger, M. Sensors, 21(21), p.6994, 2021.
6. Ciampa, F. et al. Scientific Reports, 7(1), p.14712, 2017.
7. Sherwood, G. R. et al. NDT & E International, 2021.
8. Li, W., et al. 2023. Nonlinear Ultrasonic Detection Enhanced by 3D Printed Phononic Crystals. IEEE Transactions on Instrumentation and Measurement, 2023.
9. Khalili, P. and Cawley, P. IEEE transactions on ultrasonics, ferroelectrics, and frequency control, 63(2), 303-312, 2016.
10. Aliheidari, N., et al. Polymer Testing, 60, pp.94-101, 2017.